Electrochemical degradation of the Acid Orange 10 dye on a Ti/PbO₂ anode assessed by response surface methodology

Gholamreza Bonyadinejad*, Mansour Sarafraz*, Mohsen Khosravi**, Afshin Ebrahimi*,†,
Seyed Mahmood Taghavi-Shahri***, Roya Nateghi*, and Sedighe Rastaghi****

*Environment Research Center and Department of Environmental Health Engineering, School of Health,
Isfahan University of Medical Sciences, Isfahan 81676-36954, Iran
**Nanotechnology Department, University of Isfahan, Isfahan 81744-73441, Iran
***Research Center for Environmental Pollutants, Qom University of Medical Sciences, Qom 37136-49373, Iran
****Department of Epidemiology and Biostatistics, School of Health, Isfahan University of Medical Sciences,
Isfahan 81676-36954, Iran

Abstract−The decolorization and degradation of the synthetic aqueous solution of the Acid Orange 10 (AO10) dye on Ti/PbO₂ anode were investigated using the response surface methodology based on central composite design with three variables: current density, pH, and supporting electrolyte concentration. The Ti/PbO₂ electrode was prepared by the electrochemical deposition method. The optimum conditions for AO10 decolorization in synthetic dye solution were electrolyte concentration of 117.04 mM, pH of 12.05, and current density of 73.64 mA cm^{-2}. The results indicated that the most effective factor for AO10 degradation was current density. Furthermore, the color removal efficiency significantly increased with increasing current density. To measure AO10 mineralization under optimum conditions, the chemical oxygen demand (COD) and total organic carbon (TOC) removal were evaluated. Under these conditions, decolorization was completed and 63% removal was recorded for COD and 60% for TOC after 100 min of electrolysis.

Keywords: Electrochemical Degradation, Ti/PbO₂, Acid Orange 10, Response Surface Methodology, Central Composite Design

INTRODUCTION

Textile wastewater contains potential hazardous contaminants that pollute the streams into which they are discharged. Synthetic dyes are one of the hazardous textile industry pollutants that are refractory to biological degradation [1]. Although the amount of dyes in wastewater is often lower than that of any other constituents, because of their high molar extinction coefficients, even at very low concentrations, these dyes can result in waste streams with powerful coloration [2,3].

Azo dyes are the largest group of synthetic dyes and are extensively used owing to their solubility, low cost, durability, and color diversity [4]. These dyes are persistent to biological degradation under aerobic conditions, but can be effectively degraded under anaerobic conditions. However, anaerobic treatment of textile wastewater is not suitable because the breakdown of azo dyes leads to the formation of aromatic amines, which are more toxic than the parent dye molecules and should be eliminated before the effluents are discharged into water bodies [5,6]. One of the members of the azo dyes, Acid Orange 10 (AO10), a typical azo dye in textile wastewaters [7], is a mono azo dye that is classified into the acidic dye group. According to the US National Toxicology Pro-
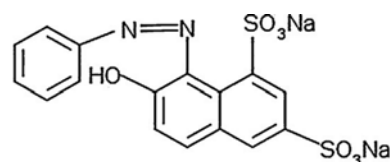

Fig. 1. Chemical structure of the azo dye AO10.

gram, until October 1966, AO10 was used as a drug and cosmetic colorant in the USA [8]. This dye has shown genotoxicity in Swiss Albino mice [9] and can also be hazardous to humans [3]. The molecular formula and molecular weight (g mol^{-1}) of AO10 are $C_{16}H_{10}N_2Na_2O_7S_2$ and 452.36, respectively [10]. The chemical structure of AO10 is shown in Fig. 1.

The conventional techniques for the treatment of dye-containing solutions are physicochemical, chemical, advanced oxidation, and electrochemical processes. Among these, electrochemical approaches, commonly performed oxidatively, have the advantage of contaminant elimination without the addition of chemicals. However, although electrochemical methods are easy to use and have high removal efficiency, energy consumption is their main disadvantage. Nevertheless, this disadvantage has been suppressed by the development of new anode materials [2,11]. Several types of electrodes, including RuO₂ [12], IrO₂ [13], Ti/TiO₂-RuO₂-IrO₂ [14], Ti/SnO₂-sb [15], PbO₂ [16], Pt-Ir [17], Pt/Ti [18], carbon nanotube [19], glassy carbon [20], Pt [21], three-dimensional electrode [22], and boron-

doped diamond (BDD) [23] have been investigated, among which PbO$_2$ is one of the best candidates [24]. PbO$_2$ is a low-cost electrode material that can be quickly and easily prepared, and is relatively stable at high applied current density (CD) and a wide range of pH [25]. During the process of oxidation of polluted waters, OH$^{\bullet}$ specimen is generated on the PbO$_2$ electrode surface, and a mechanism has been proposed for the electrochemical processes occurring in the gel-crystal structure of the PbO$_2$ layer of the electrode [26]. The Pb*O(OH)$_2$ active centers placed in the hydrated PbO$_2$ layer on the surface of the crystalline PbO$_2$ anode provide electrons to the crystal district, becoming positively charged (Pb*O(OH)$^+$ (OH)$^{\bullet}$). This electric charge is neutralized according to the following reaction:

$$Pb*O(OH)^+(OH)^{\bullet}+H_2O \rightarrow PbO(OH)_2 \ldots (OH)^{\bullet}+H^+ \qquad (1)$$

in which hydroxyl radicals are produced in the active centers. The OH$^{\bullet}$ can depart from the active centers and react with the pollutant in the aqueous solution. Thus, the PbO$_2$ anode is expected to perform quite well in organic pollutant mineralization. However, the main problem of PbO$_2$ anode is the release of poisonous ions [27]. There are several recent reports on the use of electro-oxidation to treat model aqueous solutions containing various dyes. Radha et al. [28] studied the electrochemical decolorization of AO10 with graphite rod as the anode and stainless steel as the cathode. Andrade et al. [29] examined the effect of various operating conditions on the Reactive Orange 16 dye degradation with PbO$_2$ and BDD electrodes in the anodic oxidation process.

Optimization of the operating conditions of an experimental system and recognition of the way in which the experimental parameters affect the final output of the system are realized by using modeling techniques [30]. It is also possible to determine the relationships and interactions among the variables through these techniques. In this regard, statistical methodologies, such as the response surface methodology (RSM), are suitable for studying and modeling a particular system; for example, RSM has been used for the investigation of electrochemical degradation of the Disperse Orange 29 dye [31].

As electrochemical degradation of the AO10 azo dye using Ti/PbO$_2$ anode has not yet been reported, our aim was to investigate the electrochemical oxidation of a synthetic dye solution containing AO10 using Ti/PbO$_2$ anode and determine the optimum conditions by RSM. The effects of CD, pH, and supporting electrolyte (EL) concentration were evaluated in terms of removal of color, COD, and TOC.

EXPERIMENTAL

1. Materials and Chemicals

Analytical-grade azo dye AO10 was purchased from Sigma Aldrich and used without further purification. Pb(NO$_3$)$_2$ (Sigma Aldrich), Triton X-100 (Merck), and CuSO$_4$·5H$_2$O (Merck) were used for electrode preparation. Other chemicals were purchased from Merck. The initial pH of the solutions was adjusted by using sodium hydroxide and sulfuric acid. Sodium sulfate was used as the supporting electrolyte. It has the advantage of being present usually in the dyeing bath. On the other hand, it does not involve the possibility of formation of organochlorinated compounds [32]. All the solutions

were prepared using de-ionized water.

2. Preparation of Ti/PbO$_2$ Electrode

The Ti substrate with 2 mm thickness was cut into a strip (4.8 cm×4 cm, 99.7% Aldrich) and pre-treated according to the following procedures: the substrate was polished on 320-grit paper strips [33] to eliminate the superficial layer of TiO$_2$ (an electric semiconductor) and increase surface roughness (for efficient adherence of PbO$_2$). Then, the substrate was degreased in an ultrasonic bath of acetone for 10 min and then in distilled water for 10 min. Afterwards, the substrate was etched for 1 h in a boiling solution of oxalic acid (10%) and rinsed with ultrapure water [34]. Finally, the cleaned Ti substrate was transferred to an electrochemical deposition cell, which contained 12% (w/v) Pb(NO$_3$)$_2$ solution comprising 5% (w/v) CuSO$_4$·5H$_2$O and 3% (w/v) surfactant (Triton X-100). The role of the surfactant was to minimize the surface tension of the solution for better wetting of the substrate and also to increase the adhesion of PbO$_2$ to the Ti substrate. The electrodeposition of PbO$_2$ was performed at a constant anodic current of 20 mA cm^{-2} for 60 min at 80 $^{\circ}$C with continuous stirring [35]. The X-ray diffraction (XRD) tests were performed using a Bruker Defractometer (D8 Advance, Germany). The samples were scanned under Co Kα radiation (wavelength: 1.7890 Å) at 40 kV and 40 mA. Scanning electron microscope (SEM; Philips XI30, Netherlands) was employed to observe the surface morphology of the electrodes, which presented a typical pyramid shape similar to that reported in the literature [36].

3. Electrochemical Degradation of AO10

Synthetic wastewater was prepared by dissolving AO10 in distilled water at a concentration of 100 mg L^{-1}. The electrochemical degradation of AO10 was performed in a batch reactor (0.45 L) equipped with 41.12 cm^2 Ti/PbO$_2$ as the anode and a 80.32 cm^2 stainless steel plate as the cathode in conjunction with an adjustable power supply unit (HANI, Iran) (Fig. 2). The gap between the anode and cathode was 1 cm. The duration of all the electrolysis experiments was 50 min. The reactor was placed on a magnetic stirrer for mixing its content during the experiment to maximize mass transport.

4. Analyses

The performance of electrochemical degradation was evaluated on the basis of three main factors: removal of color, COD, and TOC. The dye decoloration was monitored spectrophotometrically by
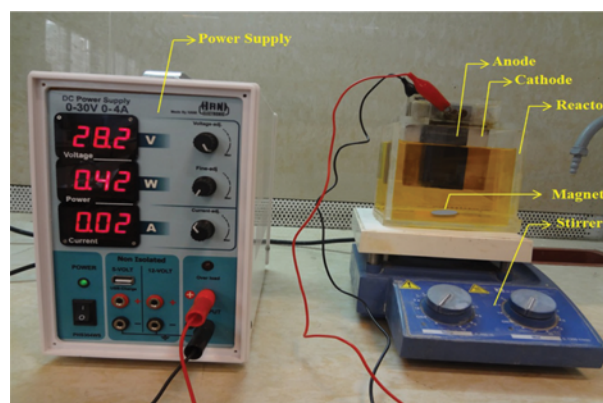

Fig. 2. Experimental setup for electrochemical degradation of AO10.

measuring the absorbance of the remaining dye at the maximum absorption wavelength (λ_{max}) of 475 nm on a UV-Vis spectrophotometer (DR-5000, HACH LANGE, USA). The amount of color removal was calculated by using the following formula:

$$\text{Color removal (\%)} = \frac{\text{ABS}_0^{475} - \text{ABS}^{475}}{\text{ABS}_0^{475}} \times 100 \qquad (2)$$

where ABS_0^{475} and ABS^{475} are the absorbances at 475 nm before and after treatment, respectively.

The COD and TOC removal were analyzed to measure the mineralization of AO10 under the optimum condition of color removal. The COD was determined colorimetrically by the dichromate method. For this purpose, an appropriate amount of the sample was introduced into a commercially available digestion solution containing potassium dichromate, sulfuric acid, and mercuric sulfate (HACH LANGE, UK), and the mixture was incubated for 120 min at 150 °C in a COD reactor (Model 45600, HACH Company, USA). A Shimadzu TOC-V$_{CSH}$ analyzer (Japan) was used to measure the TOC of the samples. The COD and TOC removal efficiencies were calculated as follows:

$$\text{COD or TOC removal (\%)} = \frac{C_0 - C_t}{C_0} * 100 \qquad (3)$$

where C_0 and C_t are the COD or TOC of the dye solution before and after electrolysis for t minutes, respectively.

For determination of initial solution resistivity (ISR), the electrical conductivity of the working solutions was measured by a portable Hach electrical conductivity meter sensION 5. Eq. (4) was used to convert electrical conductivity to resistivity for the solutions:

$$\text{ISR}_{(\Omega cm)} = \frac{1}{\text{electrical conductivity} * \text{cell constant}} \qquad (4)$$

where electrical conductivity is as siemens cm^{-1} and cell constant for electrical conductivity meter is 0.45.

5. Experimental Design

To model and determine the optimum conditions for electro-oxidation of AO10, the experimental conditions were designed by using central composite design (CCD) coupled with RSM [37], with CD, EL, and pH as the main variables. The rotatable experimental plan was performed with the three variables at five levels (−1.68, −1, 0, 1, 1.68). Table 1 shows the values and levels of the variables. Five replications were established at the center point of the design to evaluate the pure error and consequently the lack of fit. Statistica ver. 10, and R ver. 3.1.2 software were used to design and analyze the experiments. Table 2 shows the CCD matrix of the degradation experiments.

The relationship between response Y and the three independent variables X_1, X_2, and X_3 could be approximated by quadratic polynomial equation as follows:

Table 1. The range and codification of the independent variables (X_i) used in the experimental design

Variables	Actual values of the coded values				
	−1.68	−1	0	1	1.68
pH (X_1)	1.95	4	7	10	12.05
EL (mM) (X_2)	32.96	50	75	100	117.04
CD (mA cm^{-2}) (X_3)	6.36	20	40	60	73.64

Table 2. CCD matrix of electrochemical degradation of AO10

Exp. No.	pH	EL	CD	Color removal (%), Y		EC* (kWh m^{-3})	ISR (Ω·cm)
				Predicted	Observed		
1	4.00	50.00	20.00	59.10	58.87	15.15	265.50
2	4.00	50.00	60.00	100.00	95.06	70.66	265.50
3	4.00	100.00	20.00	59.10	60.30	11.48	146.78
4	4.00	100.00	60.00	100.00	96.75	58.52	146.78
5	10.00	50.00	20.00	59.70	56.08	14.39	265.18
6	10.00	50.00	60.00	100.00	95.68	70.98	265.18
7	10.00	100.00	20.00	59.70	53.39	10.64	147.36
8	10.00	100.00	60.00	100.00	95.61	57.13	147.36
9	1.95	75.00	40.00	92.99	83.39	34.69	134.68
10	12.05	75.00	40.00	94.00	90.40	35.87	172.94
11	7.00	32.96	40.00	86.86	75.14	44.7	396.12
12	7.00	117.04	40.00	86.86	80.72	33.46	130.03
13	7.00	75.00	6.36	32.15	32.32	2.24	188.16
14	7.00	75.00	73.64	100.00	96.59	81.63	188.16
15	7.00	75.00	40.00	86.86	81.87	35.7	188.16
16	7.00	75.00	40.00	86.86	82.08	32.46	188.16
17	7.00	75.00	40.00	86.86	81.16	35.65	188.16
18	7.00	75.00	40.00	86.86	80.24	36.44	188.16
19	7.00	75.00	40.00	86.86	79.70	36.11	188.16

*Energy consumption during electrolysis

$$Y = b_0 + b_1X_1 + b_2X_2 + b_3X_3 + b_{11}X_1^2 + b_{22}X_2^2 + b_{33}X_3^2$$
$$+ b_{12}X_1X_2 + b_{13}X_1X_3 + b_{23}X_2X_3 \quad (5)$$

where Y is the predicted response; b_0 is a constant; b_1, b_2, and b_3 are the linear coefficients, b_{12}, b_{13}, and b_{23} are the cross-product coefficients; and b_{11}, b_{22}, and b_{33} are the quadratic coefficients. In the present study, we used backward variable selection for multiple regression modeling. The assumption of final regression model was verified using the Anderson-Darling test for normality of residuals [38], Breusch-Pagan test for constant variance of residuals [39], and Durbin-Watson test for independence of residuals [40,41]. Lack of fit test was performed to assess the fit of the final model. Validation of the final model was established using predicted R-squares (R^2), which estimates the prediction power of the model with new observations based on the leave-one-out technique [42]. The optimum values of the final model were calculated using numerical methods. In this regard, the experimental-range predictors were divided into a grid and then the final model was calculated for all possible combinations of predictors in the grid. If the predicted response of the final model in the grid was outside of the possible range of response, it was replaced with the nearest possible value (>100% replaced with 100%) and the frequency of this problem was reported.

RESULTS AND DISCUSSION

1. Characterization of the Ti/PbO$_2$ Electrode

The XRD pattern of the Ti/PbO$_2$ electrode (Fig. 3) reveals that PbO$_2$ was deposited in the form of two known polymorphs, namely, orthorhombic α-PbO$_2$ and tetragonal β-PbO$_2$, which occur naturally as scrutinyite and plattnerite, respectively. Fig. 4 shows the SEM images of the surface microstructures of the Ti/PbO$_2$ electrode at two magnifications. It can be observed that the PbO$_2$ layer is crack free and composed of packed faceted microcrystallites. Such a morphology guarantees that only PbO$_2$ is involved in the electrochemical degradation of the dye and protects the surface of the Ti substrate. Furthermore, energy-dispersive X-ray spectroscopy (EDS) analysis (data not shown) confirmed the presence of lead and oxygen atoms on the surface of the Ti/PbO$_2$ electrode.
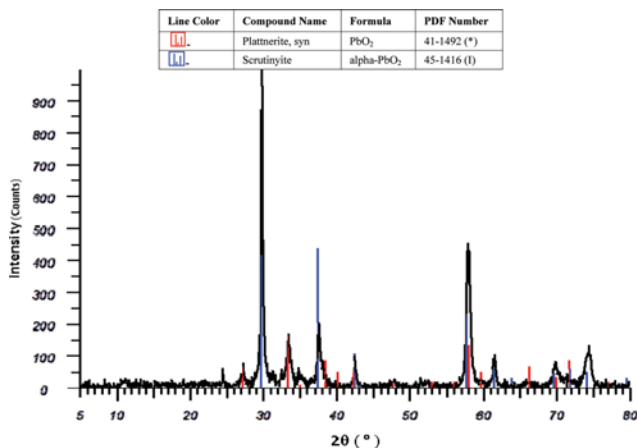

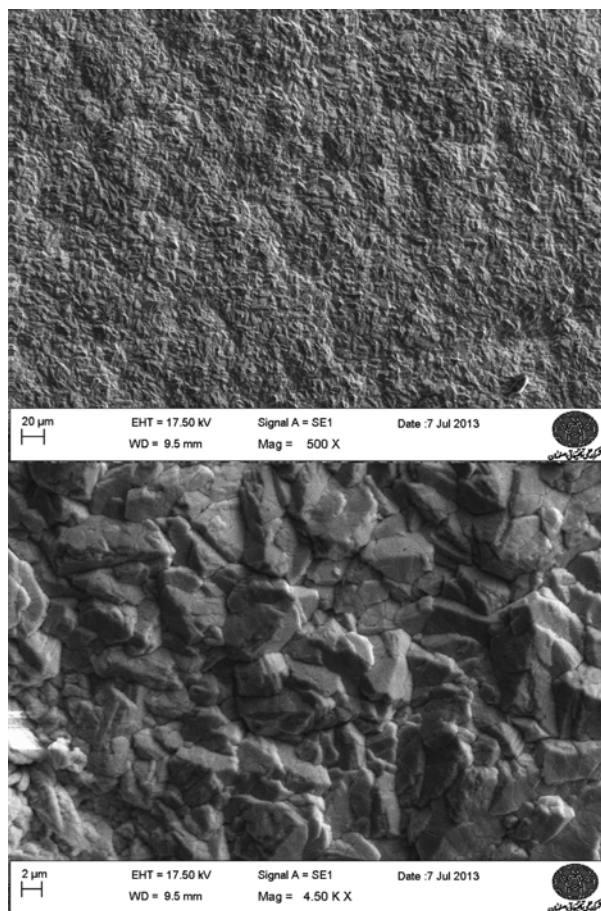Fig. 3. XRD pattern of the prepared PbO$_2$ electrode.

Fig. 4. SEM micrographs of the surface of the Ti/PbO$_2$ electrode at two magnifications.

2. CCD Analysis and Modeling

To study the combined effect of all the variables, experiments were performed with different combinations of the variables, which were statistically designed by using CCD. The CCD matrix along with the predicted and observed color removal values for the electrodegradation of AO10 are shown in Table 2. The following equation represents the first model that was developed with all linear, quadratic, and two-way interaction of predictors:
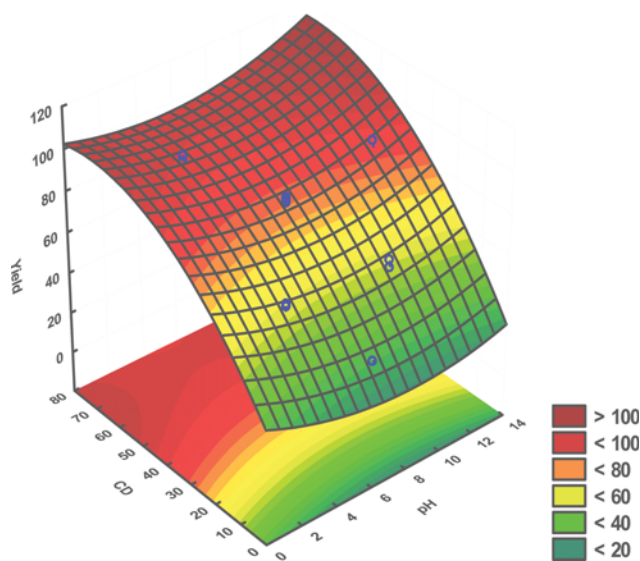
$$Y = 21.88 - 3.33X_1 + 0.31X_2 + 1.93X_3 + 0.24X_1^2 - 0.002X_3^2 - 0.014X_3^2$$
$$- 0.01X_1X_2 + 0.02X_1X_3 + 0.001X_2X_3 \quad (6)$$

The predicted R^2 of this elementary model was 0.94. No interactions of variables, linear and quadratic forms of EL, were significant. To achieve a parsimonious model with significant predictors, the interactions of the variables were removed from this model by three initial steps of backward algorithm [43]. The P-values of the EL×CD, EL×pH, and CD×pH interactions were 0.68, 0.39, and 0.18, respectively. In addition, quadratic and linear forms of the EL variable were removed by two subsequent steps of backward algorithm. The P-values of EL^2 and EL variables were 0.14 and 0.31, respectively. Thus, both the linear and quadratic forms of CD and pH variables (Table 3) were significant and were retained in the final regression model.

Table 3. Final regression model for color removal

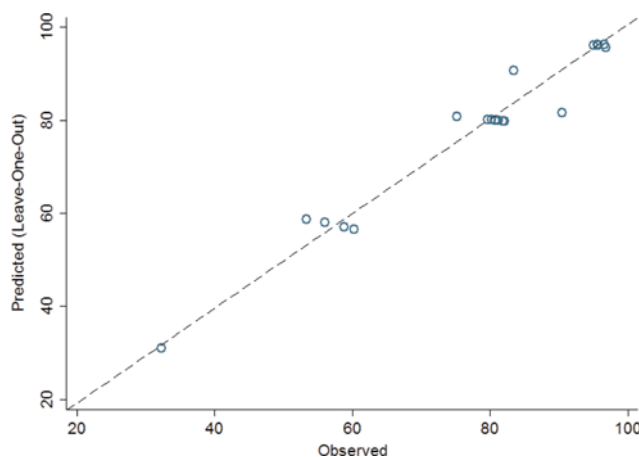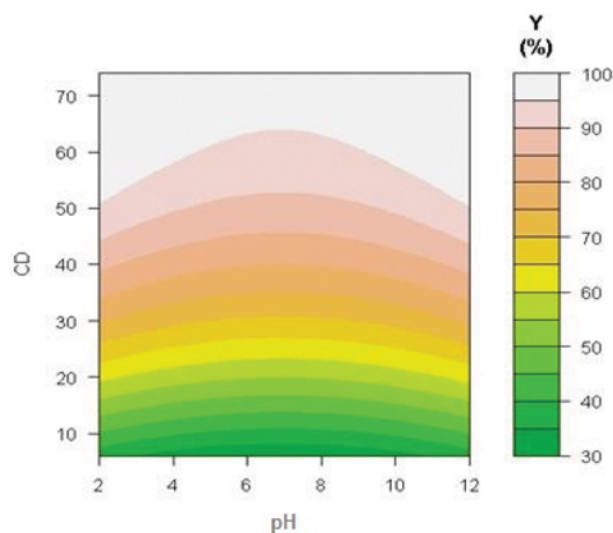| Variable	Coefficients	Std. error	T statistic	P-value
Constant value	31.288	4.634	6.752	<0.001
CD	2.088	0.139	15.038	<0.001
CD^2	−0.014	0.002	−8.371	<0.001
pH	−3.531	1.070	−3.300	0.005
pH^2	0.255	0.075	3.414	0.004

R^2=0.98, Adjusted R^2=0.98, Predicted R^2=0.96

Fig. 6. Leave-one-out prediction of the final model vs. that observed for color removal.

Fig. 5. 3D surface plot for the color removal of AO10 as a function of CD and pH.

Fig. 7. Contour plot of the final prediction model for color removal.

Table 4. Required minimum CD (mA cm^{-2}) to reach the same level of color removal

Level of color removal	pH				
	2 or 12	3 or 11	4 or 10	5 or 9	6 or 7 or 8
99%	58	64	-*	-*	-*
95%	51	55	58	61	64
90%	44	47	50	52	53
80%	34	36	38	39	40
70%	26	28	29	30	31
60%	19	21	22	23	24
50%	13	15	16	17	17

*The experimental range of CD (6-74 mA cm^{-2}) could not reach this level of response at the specified pH

Furthermore, to compare the first model with the final regression model, a partial F test was performed. The F statistic of this test was 1.08 with 6 and 9 degrees of freedom, which yielded a P-value of 0.44. Hence the difference in these two models was not significant, although the final regression model (Eq. (7)) had five predictors less than the first model (Eq. (6)). The equation of the final regression model (Fig. 5) that presented the best prediction of color removal is as follows:

$$Y = 31.30 - 3.54X_1 + 2.09X_3 + 0.26X_1^2 - 0.01X_3^2 \qquad (7)$$

Subsequently, the assumption of the final regression model was confirmed (P-values of Anderson-Darling, Breusch-Pagan, and Durbin-Watson tests were 0.28, 0.51, and 0.31, respectively). In addition, the lack of fit test was insignificant, which confirmed the fit of this model (P=0.07). The leave-one-out technique for assessing the final regression model also confirmed the external validity of this model (Predicted R^2=0.96) (Fig. 6).

As mentioned, a numerical method was used to assess the final model in the experimental range of the predictors. In this respect, the grid for a combination of pH predictors was from 2 to 12 with 0.1 increments and that for the CD was from 6 to 74 with 1 increments. Model prediction was calculated for 6969 different combinations of predictors. In 256 cases (3.7%), the predicted values were greater than 100. Hence, they were replaced with 100 because this

was the upper bound. After this adjustment, the results were plotted in a contour plot for the final prediction model, as shown in Fig. 7.

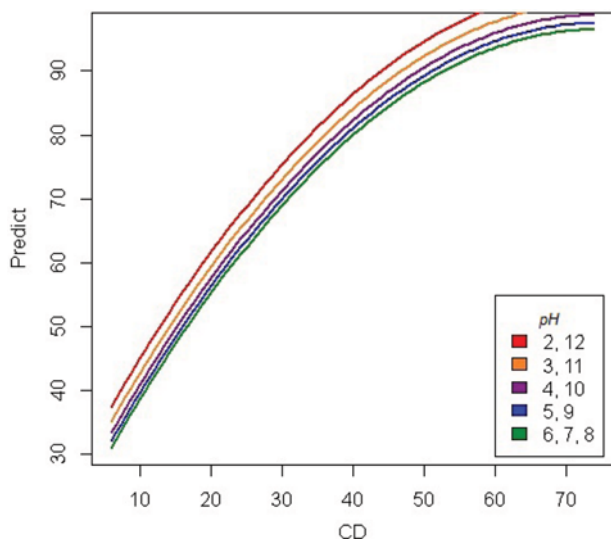As extraction of the required CD from Fig. 7 is difficult, Table 4 is

Fig. 8. Model prediction for color removal vs. CD (mA cm^{-2}) at different pH values.

provided as a simple guide to identify the minimum CD required to reach the same level of color removal. For example, Table 4 shows that the CD should be 58 and 64 mA cm^{-2} at pH 2 or 12 and 3 or 11, respectively, to achieve 99% color removal; however, at pH of 4 or 10, 99% color removal could not be achieved even with maximum CD (74 mA cm^{-2}). Fig. 8 shows the color removal that can be achieved with each value of CD. While color removal presented a positive association with CD at all pH values, when the pH was nearly neutral, complete color removal could not be achieved, even with an increase in CD.

3. Effect of Initial pH

The effect of initial pH on AO10 dye degradation was examined by adjusting the pH of the dye solutions to the following values: 1.95, 3, 7, 10, and 12.05 (Fig. 5). Despite the fact that the initial pH is an important factor in the oxidation process, the results and mechanisms are controversial owing to the diversity of the degraded dyes and electrode materials [36]. As shown in Fig. 5 and by Eq. (7), the color removal efficiency was minimum at neutral pH (6.92), and increased when the pH was acidic or basic. From Eq. (7), maximum color removal efficiency was obtained at a basic pH condition (pH=12.05). However, the rate of increase in the AO10 dye degradation was approximately the same when the pH was altered toward basic or acidic values. The difference in the color removal efficiency at pH 1.95 and 12.05 was negligible (0.38%) and was not significant. An increase in the AO10 dye degradation with the increasing pH from 6.92 can be explained by the electrochemical production of H_2O_2 in alkaline solutions [44]. Previous studies have shown that increasing the pH of the solution favored OH• formation [36], which results in higher degradation efficiency and stronger mineralization ability [45]. On the other hand, enhancement of the AO10 dye degradation efficiency under acidic pH conditions is owing to the increase in oxygen over-potential that inhibits the oxygen evolution reaction and favors the production of more potent oxidizers that are suitable for the oxidation of organic compounds [45,46]. However, in strong acidic solutions, the life of anode

decreases [47]. As a result, in the present study, a pH of 12.05 was chosen as the optimum pH value for maximum AO10 dye degradation. Eq. (7) shows that the difference between the minimum and maximum color removal efficiency related to pH is 6.57%, indicating that anodic oxidation of AO10 using PbO_2 anode is not very sensitive to the initial pH and that AO10 could be degraded under a wide pH range. Therefore, within the scope of the present study, it can be suggested that pre-adjustment of pH with the addition of chemicals is not necessary for anodic oxidation of the studied dye, unless the minute increase in the degradation efficiency is reasonable.

4. Effect of CD

We investigated the effect of CD at five levels (6.36, 20, 40, 60, and 73.64 mA cm^{-2}) in combination with pH and EL (Fig. 5). As shown in Fig. 5, which is the output of the CCD, the color removal efficiency significantly increased with the increasing CD owing to the increasing number of OH• specimen produced [46-49].

To find the optimum CD for AO10 dye degradation, Eq. (7) was independently differentiated with respect to CD (X_3) and then equated to zero, which produced a value of 104 mA cm^{-2} that was out of the experimental range. Hence, 73.64 mA cm^{-2} was chosen as the optimal value. Fig. 8 shows that the most important variable for the enhancement of AO10 dye degradation was CD.

5. Effect of EL

As described earlier, color removal was not affected by EL within the investigated range. Similar results have also been reported by many researchers [48,50,51]. However, it was found that the energy consumption (EC) significantly decreased with the increase in the EL (Table 2). Under the same condition of pH and CD, with an EL of 50 mM, the EC was 70.98 kWh m^{-3}; however, when the EL was 100 mM, the EC decreased to 57.13 kWh m^{-3}. The decrease of EC while EL was increasing can be attributed to a decrease in solution resistance. As can be seen in Table 2, under the same condition of pH and CD, with an EL of 32.96 mM, the initial solution resistivity (ISR) was 396 Ω cm, while with an EL of 117.04 mM, the ISR was 130 Ω cm, which results in EC decreases from 44.7 kWh m^{-3} to 33.46 kWh m^{-3}. These results indicated that a minimum amount of electrolyte is required to start the degradation process and addition of excess electrolyte saves energy on the condition that the highly saline effluent does not cause any adverse effect. However, some recent studies suggest the use of unlimited and clean energy sources such as solar energy that can overcome this electrochemical treatment problem [52].

6. Color, TOC, and COD Removal under Optimum Conditions

Maximum color removal efficiency was obtained under the following optimum conditions: dye concentration=100 mg L^{-1}, pH= 12.05, EL=117.04 mM, and CD=73.64 mA cm^{-2}. Under these conditions, decolorization was complete after 50 min of electrolysis. The obtained COD and TOC removal efficiencies were 40% and 28%, respectively. Moreover, the COD and TOC removal after 100 min of electrolysis were 63% and 60%, respectively. These results suggest that maximum dye removal could be achieved by increasing the electrolysis time.

CONCLUSION

Electrochemical degradation of the AO10 dye was investigated

and modeled by employing CCD coupled with RSM for the prediction and optimization of the AO10 dye removal in synthetic wastewater using Ti/PbO$_2$ as the anode and stainless steel as the cathode. The use of RSM based on CCD allowed determination of the behavior of the electrode on dye degradation, without requiring a large number of experiments, and provided sufficient information. Moreover, the CCD facilitated detecting the optimum conditions for decolorization. The final model was validated by using the leave-one-out technique, and the predicted R^2 was 0.96, which confirmed the external validity of the model. In addition, the lack of a fit test was insignificant with a P-value of 0.07, which confirmed the fit of the final model. The results of the present study demonstrated that electrochemical degradation is a suitable and environment-friendly method for the degradation of refractory dyes in aqueous solution.

ACKNOWLEDGEMENTS

ABBREVIATIONS

AO10 : acid orange 10
EC : energy consumption
CD : current density
EL : supporting electrolyte
COD : chemical oxygen demand
ISR : initial solution resistivity
TOC : total organic carbons
BDD : boron-doped diamond
SEM : scanning electron microscopy
XRD : X-ray diffraction

REFERENCES

1. A. B. dos Santos, F. J. Cervantes and J. B. van Lier, *Bioresour. Technol.*, **98**, 2369 (2007).
2. S. Mondal, *Environ. Eng. Sci.*, **25**, 383 (2008).
3. N. Jović-Jovičić, A. Milutinović-Nikolić, P. Banković, Z. Mojović, M. Žunić, I. Gržetić and D. Jovanović, *Appl. Clay Sci.*, **47**, 452 (2010).
4. M. H. Entezari, Z. S. Al-Hoseini and N. Ashraf, *Ultrason. Sonochem.*, **15**, 433 (2008).
5. S. Meriç, D. Kaptan and T. Ölmez, *Chemosphere*, **54**, 435 (2004).
6. R. Saratale, G. Saratale, J. Chang and S. Govindwar, *J. Taiwan Inst. Chem. Eng.*, **42**, 138 (2011).
7. X. R. Xu and X. Z. Li, *Sep. Purif. Technol.*, **72**, 105 (2010).
8. N. Benselka-Hadj Abdelkader, A. Bentouami, Z. Derriche, N. Bettahar and L. C. De Menorval, *Chem. Eng. J.*, **169**, 231 (2011).
9. A. K. Giri, A. Mukherjee, G. Talukder and A. Sharma, *Toxicol. Lett.*, **44**, 253 (1988).
10. S. P. Sun, C. J. Li, J. H. Sun, S. H. Shi, M. H. Fan and Q. Zhou, *J. Hazard. Mater.*, **161**, 1052 (2009).
11. C. A. Martínez-Huitle and E. Brillas, *Appl. Catal. B-Environ.*, **87**, 105 (2009).
12. S. Raghu and C. A. Basha, *J. Hazard. Mater.*, **139**, 381 (2007).
13. J. D. Rodgers, W. Jedral and N. J. Bunce, *Environ. Sci. Technol.*, **33**, 1453 (1999).
14. D. Rajkumar, B. J. Song and J. G. Kim, *Dyes Pigm.*, **72** (2007).
15. H. Xu, A. P. Li, Q. Qi, W. Jiang and Y. M. Sun, *Korean J. Chem. Eng.*, **29**, 1178 (2012).
16. J. M. Aquino, G. F. Pereira, R. C. Rocha-Filho, N. Bocchi and S. R. Biaggio, *J. Hazard. Mater.*, **192**, 1275 (2011).
17. O. J. Murphy, G. Duncan Hitchens, L. Kaba and C. E. Verostko, *Water Res.*, **26**, 443 (1992).
18. A. Vlyssides, M. Loizidou, P. Karlis, A. Zorpas and D. Papaioannou, *J. Hazard. Mater.*, **70**, 41 (1999).
19. J. Wang, R. P. Deo, P. Poulin and M. Mangey, *J. Am. Chem. Soc.*, **125**, 14706 (2003).
20. P. A. Carneiro, M. E. Osugi, C. I. S. Fugivara, N. Boralle, M. Furlan and M. V. B. Zanoni, *Chemosphere*, **59**, 431 (2005).
21. M. Sanroman, M. Pazos, M. Ricart and C. Cameselle, *Chemosphere*, **57**, 233 (2004).
22. Y. Xiong, P. J. Strunk, H. Xia, X. Zhu and H. T. Karlsson, *Water Res.*, **35**, 4226 (2001).
23. V. Santos, A. Morão, M. J. Pacheco, L. Ciríaco and A. Lopes, *J. Environ. Eng. Manage.*, **18**, 193 (2008).
24. J. Cao, H. Zhao, F. Cao, J. Zhang and C. Cao, *Electrochim. Acta*, **54**, 2595 (2009).
25. C. Comninellis and G. Chen, *Electrochemistry for the Environment*, Springer (2010).
26. M. Panizza and G. Cerisola, *Chem. Rev.*, **109**, 6541 (2009).
27. E. M. Siedlecka, S. Stolte, M. Gołębiowski, A. Nienstedt, P. Stepnowski and J. Thöming, *Sep. Purif. Technol.*, **101**, 26 (2012).
28. K. Radha, V. Sridevi, K. Kalaivani and M. Raj, *Desalin. Water Treat.*, **7**, 6 (2009).
29. L. S. Andrade, T. T. Tasso, D. L. da Silva, R. C. Rocha-Filho, N. Bocchi and S. R. Biaggio, *Electrochim. Acta*, **54**, 2024 (2009).
30. D. C. Montgomery, *Design and analysis of experiments*, 7th Ed., John Wiley & Sons, New York (2009).
31. J. M. Aquino, R. C. Rocha-Filho, N. Bocchi and S. R. Biaggio, *J. Environ. Chem. Eng.*, **1**, 954 (2013).
32. A. Fernandes, A. Morao, M. Magrinho, A. Lopes and I. Gonçalves, *Dyes Pigm.*, **61**, 287 (2004).
33. A. Polcaro, S. Palmas, F. Renoldi and M. Mascia, *J. Appl. Electrochem.*, **29**, 147 (1999).
34. A. Del Río, M. Benimeli, J. Molina, J. Bonastre and F. Cases, *Int. J. Electrochem. Sci.*, **7**, 13074 (2012).
35. N. A. Ghalwa, M. Gaber, A. M. Khedr and M. F. Salem, *Int. J. Electrochem. Sci.*, **7**, 6044 (2012).
36. L. Xu, Z. Guo, L. Du and J. He, *Electrochim. Acta*, **97**, 150 (2013).
37. R. H. Myers, D. C. Montgomery and C. M. Anderson-Cook, *Response surface methodology: Process and product optimization using designed experiments*, Wiley (2009).
38. T. W. Anderson and D. A. Darling, *J. Am. Stat. Assoc.*, **49**, 765 (1954).
39. T. S. Breusch and A. R. Pagan, *Econometrica*, **47**, 1287 (1979).
40. J. Durbin and G. S. Watson, *Biometrika*, **37**, 409 (1950).
41. J. Durbin and G. S. Watson, *Biometrika*, **38**, 159 (1951).

42. B. Efron and G. Gong, *Am. Stat.*, **37**, 36 (1983).

43. M. H. Kutner, C. Nachtsheim and J. Neter, *Applied linear regression models*, McGraw-Hill/Irwin (2004).

44. C. Zhang, Y. Jiang, Y. Li, Z. Hu, L. Zhou and M. Zhou, *Chem. Eng. J.*, **228**, 455 (2013).

45. Q. Dai, H. Shen, Y. Xia, F. Chen, J. Wang and J. Chen, *Sep. Purif. Technol.*, **104**, 9 (2013).

46. J. Niu, D. Maharana, J. Xu, Z. Chai and Y. Bao, *J. Environ. Sci.*, **25**, 1424 (2013).

47. C. Zhong, K. Wei, W. Han, L. Wang, X. Sun and J. Li, *J. Electroanal. Chem.*, **705**, 68 (2013).

48. M. Zhou and J. He, *J. Hazard. Mater.*, **153**, 357 (2008).

49. N. Djafarzadeh, M. Safarpour and A. Khataee, *Korean J. Chem. Eng.*, **31**, 785 (2014).

50. J. Niu, Y. Bao, Y. Li and Z. Chai, *Chemosphere*, **92**, 1571 (2013).

51. D. Shao, J. Liang, X. Cui, H. Xu and W. Yan, *Chem. Eng. J.*, **244**, 288 (2014).

52. E. Alvarez-Guerra, A. Dominguez-Ramos and A. Irabien, *Chem. Eng. Res. Des.*, **89**, 2679 (2011).